

Design and Testing of a Cosmic Ray Shielding Scintillator Array for the Proposed MECO Experiment

Chris Neilson

Physics 451 Senior Research

The College of William and Mary

April 14, 2000

Design and testing of a cosmic ray shielding scintillator array for the proposed MECO experiment

Introduction

MECO, standing for Muon to Electron Conversion, is a proposed experiment to test supersymmetric extensions to the Standard Model by looking for the violation of the lepton flavor conservation law. If accepted MECO will run at the Alternating Gradient Synchrotron accelerator at Brookhaven National Laboratory. Searching for lepton flavor nonconservation at a sensitivity of 1 part in 10^{16} , it becomes extremely important to minimize background radiation. One type of background, cosmic rays (CR), will be shielded against by a scintillator array that will surround the experimental detectors.

The purpose of the scintillator array is to veto the recording of any event triggered by a CR particle in MECO's detectors. The array will achieve this objective by using scintillator embedded with wavelength-shifting fibers. Such a system is described in depth by Wojcik *et al.*¹ and is employed in the MINOS experiment². The goal of this research is to improve upon the system in a way that can be incorporated into MECO, by testing novel configurations and improved materials and hardware.

Background

MECO will search for the muon conversion process. The process involves a negative muon in the 1S atomic state converting to an electron in the field of the nucleus ($\mu^- + N \rightarrow e^- + N$). The resulting electron has a kinetic energy of 105 MeV, the difference in rest mass between the muon and the electron. The electron escapes the nucleus, which recoils, conserving momentum. Because no neutrinos are produced, muon conversion violates the lepton flavor conservation law which demands that the number of leptons from a given family be conserved.

Violation of the lepton flavor conservation law has never been observed. The Standard Model does not describe a cause for violation of the law, however, it is also silent regarding a reason for lepton flavor conservation. Extensions to the Standard Model such as supersymmetry require the absence of a lepton conservation law. Thus, MECO could provide an empirical test to Standard Model extensions.

The MECO experiment, shown schematically in Fig. 1, is designed to send a μ^- beam at an aluminum target. As the muons traverse the aluminum they lose energy through Coulombic interactions, finally coming to rest within the target. Before decaying, it is possible for a negative muon to displace an electron in an aluminum atom. The muon quickly falls to the muonic 1s orbital. It is in this state that muon conversion will occur—if the process exists.

The beam of muons is created, through a series of steps, from an 8 GeV proton beam. The protons are shot at a tungsten target, producing pions. Pions decay into muons with an almost 100% branching ratio. This occurs within the superconducting production solenoid which has an intense magnetic field. This field forms a gradient

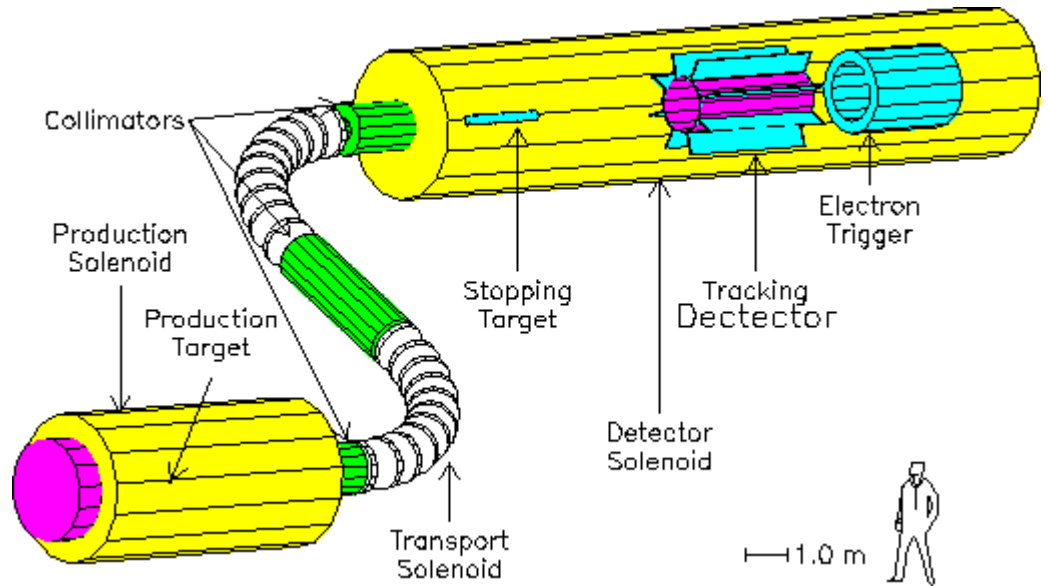


Figure 1 Simplified picture of MECO beam lines showing production, transport and detector solenoids. Picture courtesy of MECO collaboration³.

from 3.3 T to 2.0 T, designed to direct charged particles into the transport solenoid. Within the transport solenoid, positively charged particles are filtered out as well as negative pions, leaving a beam of negative muons. The transport solenoid delivers this beam to the detector solenoid which contains the aluminum target and the experiment's detectors.

Previous experiments searching for muon conversion have been conducted, reaching a maximum sensitivity of 6.1×10^{-13} with SINDRUM II⁴. As proposed, MECO is expected to reach a sensitivity of 10^{-16} . The increased sensitivity will be due mainly to an improved muon beam. The beam, to be developed at the AGS, will have an intensity of 10^{11} muons/sec, an increase over the previous experiments by approximately four orders of magnitude.⁵

Due to the great sensitivity of the experiment, background radiation can cause a serious problem. Cosmic rays are one source of such background. GEANT simulations have shown that CR-induced background can be reduced to acceptable levels if both active and passive shielding are employed along with certain selection criteria.⁵ The active shielding consists of a scintillator veto counter which will form two layers around the detector. The efficiency of the counter must be 99.99%.⁵ Such a high efficiency in the counter calls for special considerations to be made in the design.

Cosmic Rays and Cosmic Ray Shielding

The composition of CRs incident on the Earth is 87% protons and 13% neutrons, with the neutrons being bound to nuclei. These nucleons interact with molecules in the atmosphere producing secondary particles, the bulk of which are pions and kaons. Assuming these particles don't interact further, pions and many kaons will decay into muons. Under such conditions, 75% of all CRs reaching sea-level are muons. The intensity of CR muons at sea-level is $1.1 \times 10^{-2} \text{ cm}^{-2} \text{ sec}^{-1} \text{ sr}^{-1}$ compared to a flux of $1.5 \times 10^{-5} \text{ cm}^{-2} \text{ sec}^{-1} \text{ sr}^{-1}$ for protons.⁶ The muon flux at sea-level has an average energy of 2 GeV. At such energies muons are highly penetrating, therefore, it is important to consider cosmic ray muons in designing shielding for the MECO experiment.

The detector solenoid of the MECO experiment will be completely surrounded by the cosmic ray shield.⁵ The outer, passive shielding will consist of concrete and steel. The outer layer will largely eliminate the penetration of most particles except muons and neutrinos. Neutrinos interact with matter at a negligible rate leaving muons as the prime source of cosmic ray background. Cosmic muons entering the detector solenoid can be

mistaken for electrons or produce them by way of secondary mechanisms. The active shielding provides a system that can veto events triggered by muons.

The bulk of the active shielding will be plastic scintillator. The plastic scintillator consists of long polymer chains containing aromatic hydrocarbons that form π -molecular orbitals. π -electrons fill these orbitals and those that are free valence electrons become delocalized over the molecule. The π orbitals have ground states (S_0) and excited states (S^* -- first excited state, S^{**} -- second excited state, etc.). Each state also has a fine structure caused by excited vibrational modes of the molecule. The vibrational states are of higher energy than the S state they are associated with and are separated by energies on the order of tenths of an eV.

A charged particle traversing the scintillator loses energy through elastic scattering with nuclei and through inelastic collisions with the delocalized electrons. An inelastic collision typically ionizes the electron, which decays to S^* within 10 ps. This occurs through non-radiative processes called internal degradation. From the S^* state, the electron has a high probability of decaying with photon emission to one of the S_0 vibrational states. The photon emitted by this transition is of lower energy than what is required to excite an electron from S_0 to S^* , thus making the scintillator transparent to the light it emits. By coupling a photomultiplier tube (PMT) to the scintillator, the photons can be detected and serve as a signal that a charged particle has crossed the scintillator.

As part of MECO's shielding, scintillator will come in "boards" with dimensions 6.5 m long x 10 cm wide x 1 cm thick, except for the end pieces which will be 4 m long. Fifteen hundred of these boards will form a box around the detector solenoid.⁵ As mentioned above there will be two layers of scintillator. This arrangement is necessitated

by the desired efficiency of 99.99%. If only a single layer were used, the spaces between boards would allow a path for a cosmic ray to follow which would not traverse the scintillator. By staggering the second layer with respect to the first, all incident particles would traverse at least one layer of scintillator. To achieve the 99.99% shielding efficiency, it is necessary for each layer of the active shielding system to be 99.9% efficient.

Another component of the active shielding is wavelength-shifting fibers (WSFs). The name WSF is explanatory of its function. The fiber absorbs light at one wavelength and fluoresces light at a longer wavelength, similar to the mechanism of scintillator fluorescence. The WSFs used in MECO will shift the blue light emitted by the scintillator to green light. In the MECO design, straight grooves are cut into the surface of a scintillator board that run the length of the board. A WSF is glued into each groove as shown in Fig. 2.

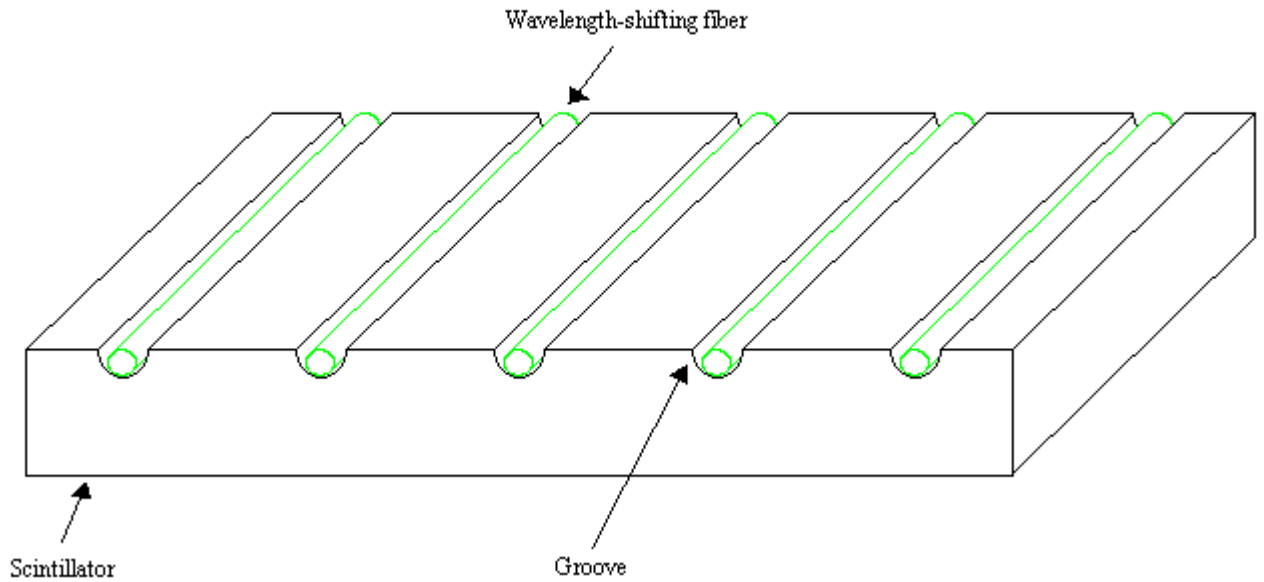


Figure 2 Grooved scintillator with embedded wavelength-shifting fibers.

When a particle causes the scintillator to fluoresce, photons are produced that travel through the scintillator. As a photon approaches the surface of the scintillator, confinement of the photon within the scintillator depends on the angle of incidence of the photon being less than a critical angle determined by the indices of refraction of the scintillator and air. Wrapping the scintillator in a reflective material allows partial recovery of photons exiting the scintillator. As photons travel through the scintillator, they may encounter a WSF, entering it. Once inside the fiber, the blue photons' wavelengths are shifted and the resulting green photons are transported to either end of the fiber as illustrated in Fig. 3. Photomultiplier tubes (PMTs) then read the output of the WSFs instead of the scintillator. In the MECO experiment, a WSF will lead to a PMT at both ends of the fiber and the signals from will be summed to attain the maximum possible output.

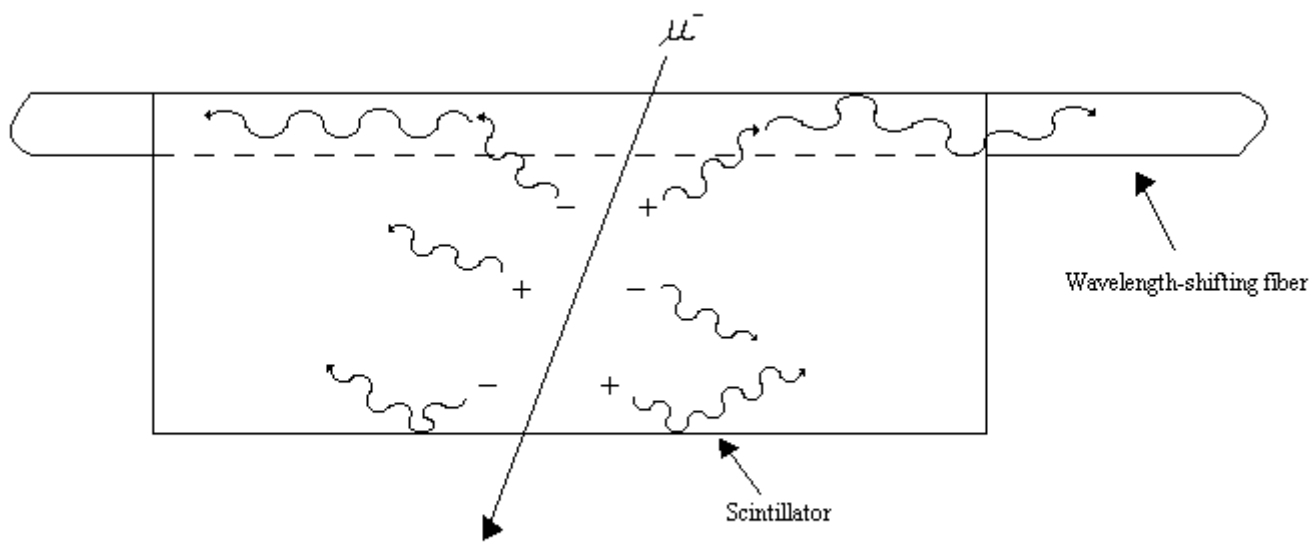


Figure 3 A cosmic muon causes the scintillator to fluoresce blue photons. Blue photons that enter the WSF are shifted to green photons and travel down the fiber to PMTs at both ends.

Incorporating WSFs into the scintillator offers many advantages over scintillator alone. Characteristics such as attenuation length, response uniformity, and ease of manufacturing are enhanced.¹ The scintillator and WSF are largely transparent to the light they fluoresce. This is what allows transport of the photons through the material. However, WSF is more transparent to its fluorescence than scintillator. This makes the attenuation length of WSF greater. In a scintillator-WSF system, the attenuation length is determined by the WSF.¹ The greater attenuation length results in greater signal output over long distances, which is critical when dealing with scintillator lengths as prescribed by the MECO proposal. In considering uniformity of response there is both longitudinal and transverse uniformity to consider. Using a 4 meter Bicron BC-408 scintillator with 6 meter Bicron BCF-92 WSFs with readout at both ends, summed signals with less than

10% variation over the length of the scintillator can be obtained.¹ Transverse uniformity is dependent on the number of WSFs and spacing between the fibers.¹

Experimental Setup

Testing was performed on a length of Bicron BC-408 scintillator with dimensions 89.3 cm x 9.85 cm x 0.973 cm. Bicron BCF-92 waveshifting fibers were embedded in 2 mm deep grooves running the length of the scintillator. A total of five fibers were spaced 2 cm from each other beginning 1 cm in from either edge. At one end of the scintillator labeled S1 in Fig. 4, the fibers extended beyond the scintillator by 1 m, their ends bundled and terminating on the face of a Hamamatsu R580-17 PMT. On the other end, the fibers were flush with the scintillator and terminated at a reflective endcap. Thus, photons arriving at this end of the fibers were reflected towards the PMT. The scintillator was then wrapped in white Tyvek paper to prevent light leakage and thus increase output.

The Hamamatsu R580-17 PMT was placed in a mu metal tube to reduce the effects of the Earth's magnetic field. Inside the mu metal tube, at the face of the PMT, the magnetic field was measured to be 0.019 Gauss using the F.W. Bell 9500 digital gaussmeter. The R580-17 is a bialkali PMT with a 38 mm (1-1/2 inch) diameter photocathode. It has a number of characteristics well suited for this experiment. For example, the PMT has a maximum efficiency for photons at 420 nm making it especially sensitive to the green light delivered by the WSFs.

In addition, the PMT can detect a single photoelectron. Single photoelectrons are often associated with noise generated by the PMT itself, however, knowing the spectrum of a single photoelectron allows one to determine the number of photoelectrons associated with signals in other spectra. A measure of the number of photoelectrons can

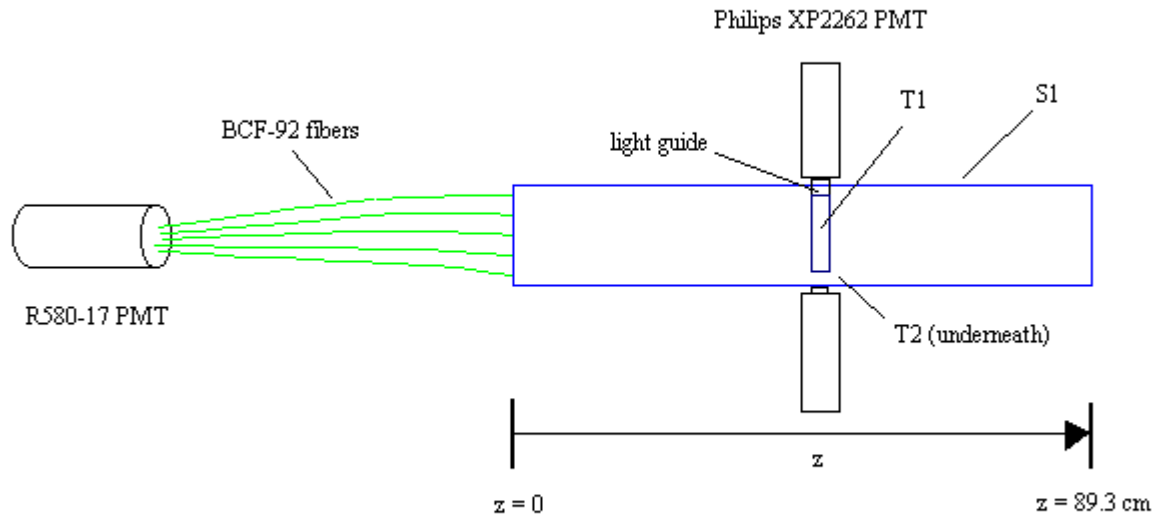


Figure 4 Top view of experimental setup for measuring attenuation length of the fiber-embedded scintillator. Two “trigger sticks”, T1 and T2, are located on either side of the BC-408 scintillator (T1 above and T2 below) so that they overlap. The sticks are perpendicular to the z-axis along the length of the scintillator. The sticks can be moved to different distances from the end of the scintillator.

be interpreted as the strength of a signal and hence offers a means by which to measure signal intensity.

A triggering system⁷ was necessary in order to count events caused by CRs but exclude those due to other sources of background and noise. Triggering was achieved by using an additional two polystyrene scintillators labeled T1 and T2 in Fig. 4. These “trigger sticks” each have one end which lead to cylindrical light guides and then on to Philips XP2262 PMTs. The sticks are positioned, one above the fiber-embedded scintillator and one below, so that they overlap each other and are perpendicular to the

fiber-embedded scintillator. Signals from both trigger sticks which coincide in time are used as a gate signal allowing output from the fiber-embedded scintillator to be recorded. This geometry creates a situation in which virtually all events recorded will be caused by a single charged particle traveling through all three scintillators. Further, the small solid angle through which a charged particle must pass to cross all three scintillators, combined with the amount of energy a particle would lose by its passage, eliminates background due to radioactive decays in the immediate surroundings. The triggering method has the added benefit of excluding most tube noise from any spectrum taken.

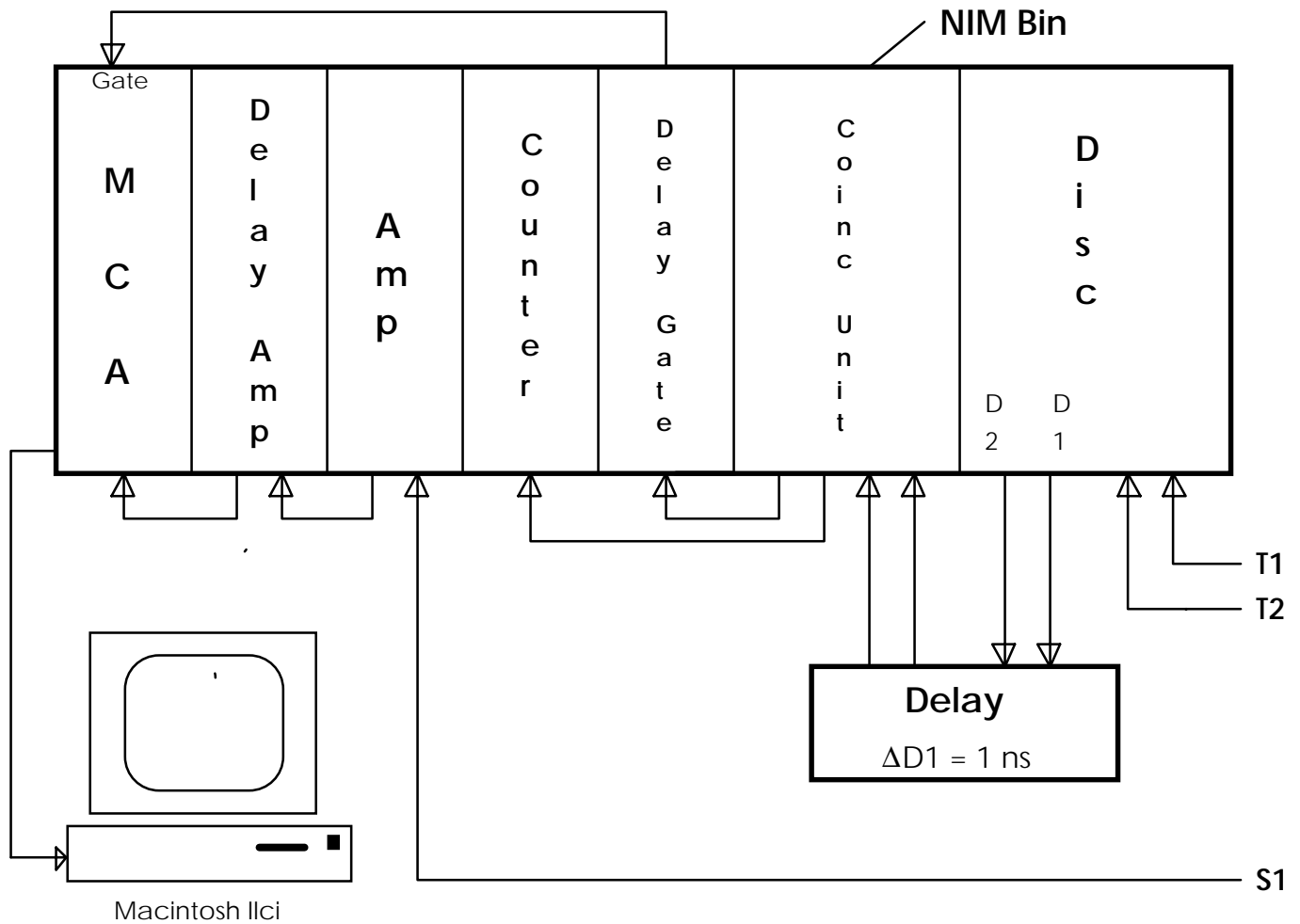
A small number of accidental gates will be triggered when two particles, one in both trigger sticks, are detected within a period of time less than the time resolution of the triggering system. During one of these accidental gates it is possible for background or noise to be counted as if it were a CR-induced event. The rate at which such accidentals occur, R_{ac} , can be calculated by the equation

$$R_{ac} \cong \sigma N_1 N_2$$

where σ is the time resolution and N_1 and N_2 are the rates at which single events are detected in T1 and T2, respectively.⁷ Measurements give $N_1 = 5.07$ counts/sec and $N_2 = 8.27$ counts/sec. Time resolution is determined by the widths of the two signals after passing through a discriminator. Using an EG&G T105/N discriminator, signal widths were set at $w_{T1} = 11$ ns and $w_{T2} = 16$ ns. The sum of the two widths determines time resolution, so $\sigma = 27$ ns. Therefore, the triggering system was susceptible to accidentals at the rate of 1.1×10^{-6} counts/sec. With a coincidence rate of 0.12 counts/sec, accidentals account for roughly 9.2×10^{-4} % of the coincidences detected by the triggering system.

Detection of coinciding events (coincidences) in the trigger sticks, as well as using this criterion as a gate for readout of S1, was accomplished by use of the electronic logic circuits diagramed in Fig. 5. NIM standard electronics units were used to build the necessary circuits.

The signal from an event was sent to a Tennelec TC 241 amplifier to increase gain and then to a delay amplifier to coordinate signal timing with the gate, before being read by an Oxford multichannel analyzer (MCA). Data from the MCA was then sent to a computer for analysis.



- MCA = Tennelec/Nucleus Oxford Multichannel Analyzer
- Delay Amp = Ortec 427A Delay Amplifier
- Amp = Tennelec TC 241 Linear Amplifier
- Counter = Ortec 772 Counter
- Delay Gate = EG&G Model GD105/N Delay Gate
- Coinc Unit = Phillips Scientific Model 754 Coincidence Unit
- Disc = EG&G T105/N Dual Discriminator
- Delay = Chronetics Inc. Model 21 Dual Delay
- NIM Bin = Tennelec TB 3 NIM Bin

Figure 5 Electronics used to readout the signal from S1 triggering on coincidences in T1 and T2.

Results

An ungated spectrum was initially taken to characterize the tube noise.

This spectrum is displayed in Fig. 6. The peak corresponds to the single photoelectron noise. The data was fit to a gaussian, the values m_1 through m_4 seen in Figure 6 represent the parameters of the gaussian

$$y = m_1 + m_2 \cdot e^{-(x-m_3)^2/(2m_4^2)}$$

The centroid channel is found to be 4.72 with an error of +/- 0.03 channels. It is now a simple matter to convert the spectrum from number of channels to number of photoelectrons, N_P , by dividing the channel number, N_C , by the 4.72 channels associated with a single electron

$$N_C / 4.72 = N_P$$

Plotting the spectrum versus the number of photoelectrons can be seen in Figure 7.

A test was done to determine the average number of photoelectrons present in signals induced by cosmic rays. Placing the trigger sticks near the middle of the scintillator at the $z = 49.6$ cm position, a spectrum was taken and fit giving an average of 7.14 +/- 0.08 photoelectrons, as shown in Fig. 8.

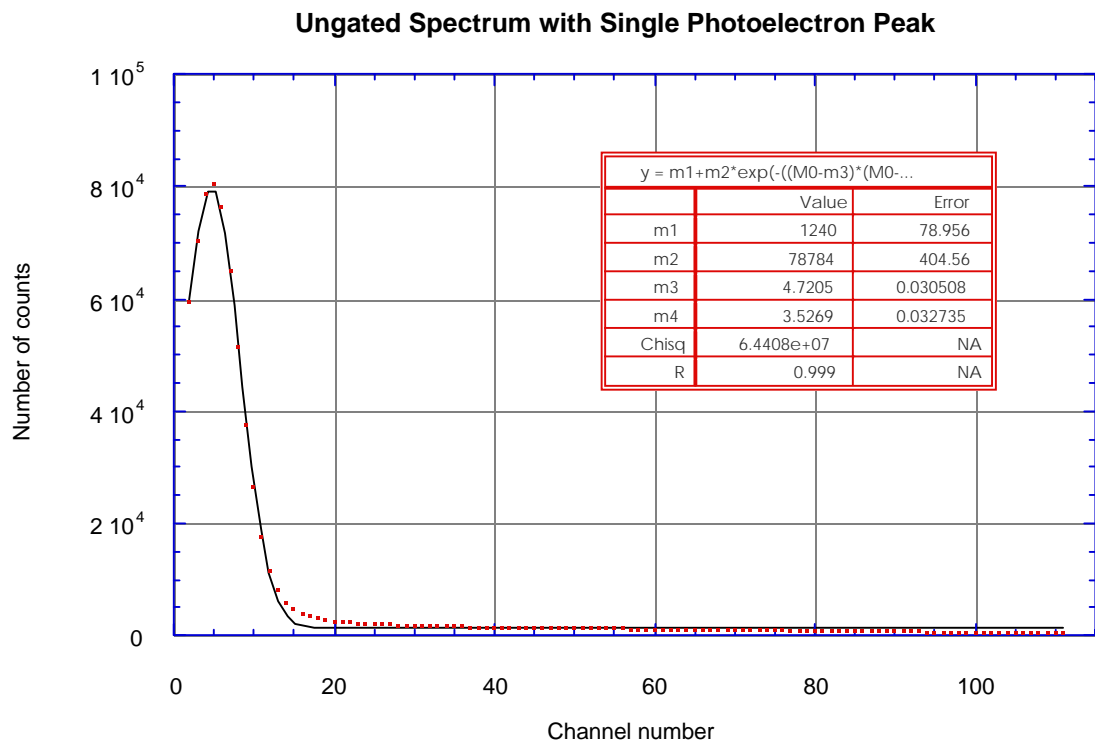


Figure 6 An ungated spectrum from S1. The peak corresponds to noise in the R580-17 photomultiplier tube generated by single photoelectrons coming off the photocathode. The peak has a centroid at 4.72 ± 0.03 , associating single photoelectrons with this channel number.

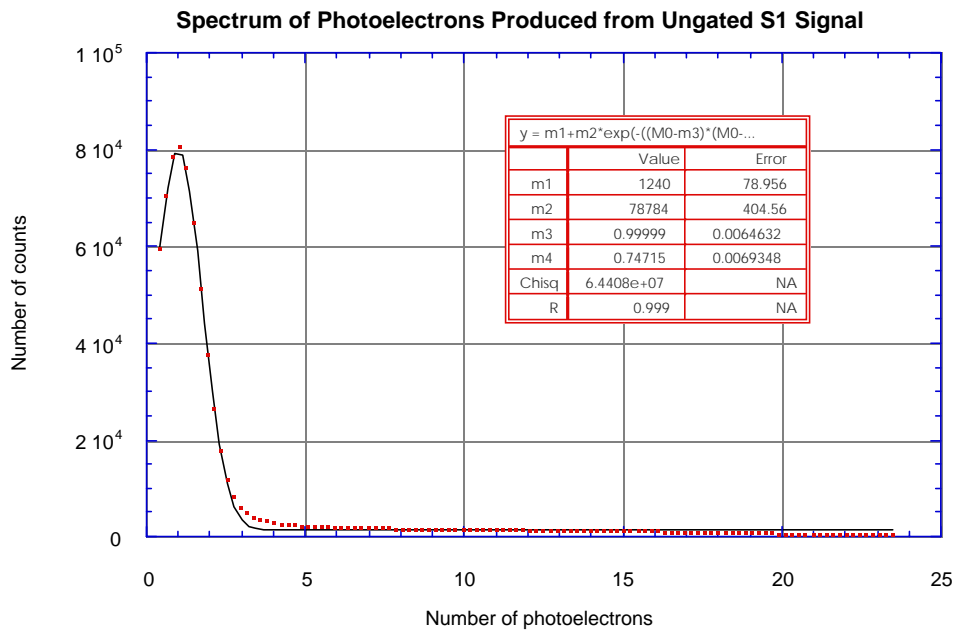


Figure 7 This graph contains the same data as in Fig. 6 but is replotted with number of photoelectrons along the x-axis. The centroid now occurs at $x = 1.0$.

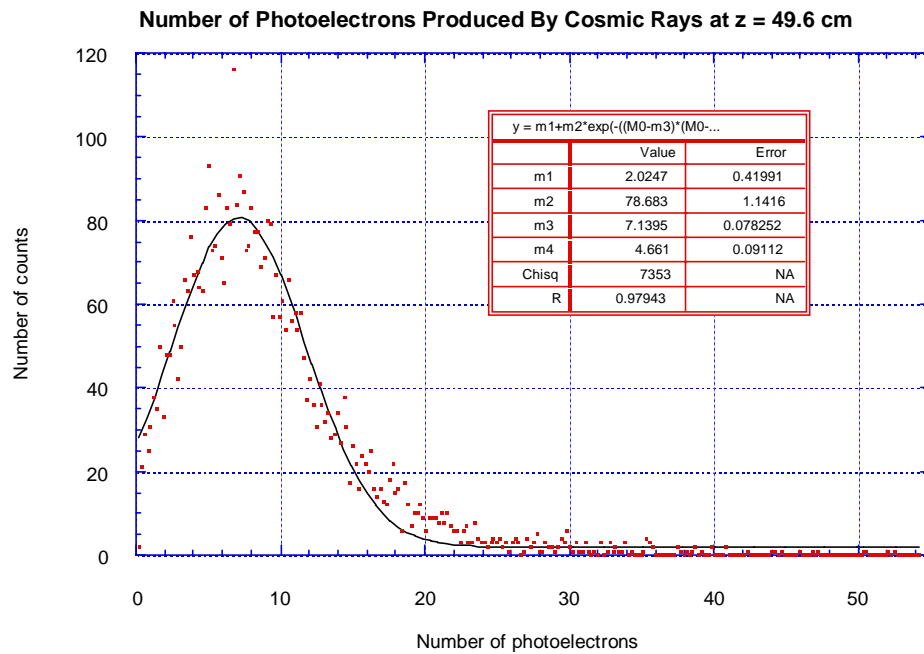


Figure 8 Number of photoelectrons produced from events at $z = 49.6$ cm. T1-T2 coincidences were used to gate the S1 signal.

Next, a test was done to determine whether the simple addition of optical grease at the WSF-PMT interface would increase the number of photoelectrons detected. The result was an increase of 34%, giving an average signal intensity of 9.58 ± 0.12 photoelectrons.

Continuing to use optical grease, studies of the number of photoelectrons detected by triggering at different points along the z-axis were initiated. Data is shown in Table 1. An inspection of the data set reveals a substantial drop off in the number of photoelectrons produced from events occurring near either end of S1. The cause for these edge effects is unknown at this time.

z (cm)	Photoelectrons	Error
1.9	5.72	0.11
28.3	9.09	0.11
49.6	9.58	0.12
59.4	9.65	0.11
69.3	9.00	0.08
79.3	9.44	0.10
86.4	7.83	0.09

Table 1 Number of photoelectrons detected versus distance along the z-axis of S1. T1 and T2 were centered at z and the S1 signal were gated on T1-T2 coincidences. The data were collected using optical grease to couple the WSFs to the PMT.

With the above data, the attenuation length ℓ can be found by the equation

$$L(z) = L_0 e^{-(z/\ell)}$$

where $L(z)$ is the light intensity and L_0 is the initial light intensity.⁷ The number of photoelectrons is proportional to the number of photons hitting the photocathode of the PMT, thus the number of photoelectrons may be used as a measure of the intensity. The data in Table 1, however, did not provide an acceptable fit to the equation for attenuation length.

Discussion

Employing optical grease to couple the WSF ends to the face of the PMT significantly increases photoelectron output. In the actual MECO experiment, the WSFs would be glued onto the face of the PMT. Adhering fibers to the PMT has the same effect as optical grease, assuming the glue is transparent to green light. Thus, the increased efficiency seen by using optical grease may be expected to be incorporated into the MECO detectors.

An attenuation length could not be determined. This is to be expected, however, as similar systems have attenuation lengths of over 5 m,¹ making the measurement extremely difficult in the short length of the WSF-embedded scintillator. The reflective endcap found on the end of the scintillator is also problematic in measuring attenuation length. This arrangement potentially allows a single event to produce photons which, in order to reach the PMT, have a difference in length of travel equal to twice the length of the scintillator. Attempts to measure attenuation length using 3.5 m long WSFs and a movable segment of grooved scintillator may be forthcoming.

The reduced photoelectron count observed from CR events at the ends of S1 are of concern. It is necessary to understand the reasons for such losses and explore ways to prevent them as the losses will adversely affect the efficiency of the CR shielding scintillator.

Signal intensity measured from events occurring along the mid-section of S1 ranged from 9.0 – 9.65 photoelectrons. Based on performance of similar WSF-scintillator systems used in MINOS, MECO collaborators expect to obtain outputs of 8-12 photoelectrons, and that such outputs will be more than sufficient to obtain the 99.99%

efficiency required of the scintillator shielding⁵. Our results fall within this range however, the results were obtained using scintillator only 0.893 m long, which is far short of the 6.5 m lengths to be used in MECO. Increasing the length of the WSF-scintillator system to this scale may cause attenuation to become significant, reducing photoelectron output below the expected range. Further attenuation length measurements are necessary to resolve this issue.

As the studies done by Wojcik *et al.* were done in 1993, there may be newer materials or equipment available which could improve the scintillator-WSF system. For example, Hamamatsu has developed a new PMT, the H7421-40, with a quantum efficiency of 40% for green light.⁸ This is an improvement by a factor of two over the R580-17. Furthermore, novel configurations of embedding the WSFs may prove to yield more efficient detectors.

Conclusion

MECO will search for violation of lepton flavor conservation in the form of muon conversion at a sensitivity of 10^{-16} . In order to exclude cosmic ray background, passive and active shielding will be employed. The active shielding will consist of scintillator embedded with wavelength-shifting fibers. The scintillator-WSF shielding system offers advantages over scintillator alone including an increased attenuation length, a critical characteristic because of the long scintillator boards used in MECO. Improvements can be made to the fiber-embedded scintillators, however. We have begun research that will incorporate new materials and hardware as well as novel configurations of the fiber-embedded scintillators. These experiments should yield improvements to the efficiency of the scintillator-WSF systems and which could be utilized in the MECO experiment.

Acknowledgements

Foremost, I would like to recognize Dr. John Kane. His knowledge and guidance were invaluable to the success of the project. Stan Majewski, Randy Wojcik, Carl Zorn, and Brian Kross of the Jefferson Lab detector group loaned equipment and provided consultation also vital to the project. I thank Andrew Norman for offering helpful suggestions and showing me a masterful way to wrap scintillator. Finally, thanks go to John Bensel, Mel Woods, and the rest of the machine shop staff for machining scintillator and lending advice on working with plastics.

References

1. Wojcik, R. *et al.* "Embedded waveshifting fiber readout of long scintillators". Nuclear Instruments and Methods in Physics Research A. 342. 1994. 416-435.
2. MINOS Technical Design Report v1.0. Oct. 15, 1998. Found on World Wide Web at http://www.hep.anl.gov/ndk/hypertext/minos_tdr.html. Dec. 2, 1999, 16:41 EST.
3. Found on World Wide Web at <http://meco.ps.uci.edu/>. Apr. 14, 2000, 15:23 EST.
4. Dohmen, C. *et al.* "Test of lepton-flavour conservation in $\mu \rightarrow e$ conversion on titanium". Physics Letters B. 317. 1993. 631-636.
5. Molzon, W. *et al.* "A search for $\mu N \rightarrow e N$ with sensitivity below 10^{-16} ". An MRE proposal to NSF, accepted at BNL. 1999.
6. Wolfendale, A. W. Cosmic Rays at Ground Level. London: The Institute of Physics. 1973.
7. Leo, William R. Techniques for Nuclear and Particle Physics Experiments 2nd ed. New York: Springer-Verlag. 1994.
8. Counting Photons. A newsletter from Hamamatsu Corp. March 2000, Vol. 4.